Axial load transfer for piles in sand

I: Tests on an instrumented precast pile

Ameir Altaee, Bengt H. Fellenius, and Erman Evgin

Department of Civil Engineering, University of Ottawa,
Ottawa, Ontario, Canada, K1N 6N5

ALTAEE, A., FELLENIUS, B. H., and EVGIN, E., 1992. Axial load transfer for piles in sand. I: Tests on an instrumented precast pile. Canadian Geotechnical Journal, Vol. 29, No. 1, pp. 11 - 20.

Axial load transfer for piles in sand. I. Tests on an instrumented precast pile

AMEIR ALTAEE, BENGT H. FELLENIUS, AND ERMAN EVGIN

Department of Civil Engineering, University of Ottawa, Ottawa, Ont., Canada K1N 6N5

Received December 28, 1990

Accepted August 15, 1991

A precast concrete pile was driven 11.0 m into a sand deposit and subjected to three compression and one tension static loading tests. By means of strain-gage instrumentation, the loads imposed in the pile during the tests were determined. The observed load distributions appeared to suggest the existence of a critical depth. However, when the load data were supplemented with the residual load acting before the start of the tests, the appearance of critical depth disappeared. Instead, the analysis of the tests showed that the load distribution was a function of the effective overburden stresses in the soil over the full pile length, with β-ratios ranging from 0.40 through 0.65 and a toe bearing coefficient of 30. The shaft resistance degraded slightly from test to test. The shaft resistance in tension was about equal with the shaft resistance in compression. The β-ratios and the toe bearing coefficient derived from the test were applied unchanged to the results of compression tests on a second test pile, a 15 m long identical pile, and the calculated capacity agreed with the capacity found in the static loading test.

Key words: instrumented pile, sand, loading test, residual load, load transfer.

Un pieu en béton précontraint a été foncé 11,0 m dans un dépôt de sable et soumis à trois essais de chargement statique en compression et un en tension. Les charges développées dans le pieu durant les essais ont été déterminées au moyen d'une instrumentation avec des jauges de résistance. Les distributions des charges observées semblent suggérer l'existence d'une profondeur critique. Cependant, lorsque la charge résiduelle agissant avant le début des essais a été ajoutée aux données de charges dans le pieu durant l'essai, l'apparition d'une profondeur critique a disparu. L'analyse des résultats a plutôt montré que la distribution de charge était fonction des contraintes effectives du poids des terres susjacentes dans le sol sur la pleine longueur du pieu avec des rapports β variant de 0,40 à 0,65; et un coefficient de portance à la pointe de 30. La résistance du fût s'est dégradée légèrement d'un essai à l'autre. La résistance du fût en tension était à peu près égale à sa résistance en compression. Les rapports β et le coefficient de portance à la pointe dérivés de l'essai ont été appliqués sans changement aux résultats des essais de compression sur un deuxième pieu, identique au premier et de 15 m de longueur, et la capacité calculée concordait avec celle trouvée dans l'essai de chargement statique.

Mots clés : pieu instrumenté, sable, essai de chargement, charge résiduelle, transfert de charge.

[Traduit par la rédaction]

Can. Geotech. J. **29**, 11-20 (1992)

Introduction

A pile test programme was carried out in 1984 at the Baghdad University Complex, Iraq, close to the bank of the River Tigris. An instrumented test pile consisting of a 285 mm square, precast concrete pile was driven 11.0 m into a sand deposit and subjected to three axial compression and one tension static loading tests.

The purpose of the test was to obtain information for use in the design of pile foundations for the expansion of the university campus. The test was influenced by the presence of residual load in the pile, and the paper demonstrates how to analyze the results to determine the amount of residual load and the true load distribution in the pile. The analysis produces the soil parameters controlling the pile capacity. These parameters are then used to extrapolate the results to piles of different size and length at the site.

Soil profile

The soil profile next to the test pile location consisted of two main soil layers: one upper, 3.0 m layer of clayey silty sand deposited on a lower, thick layer of uniform sand with some silt. Figure 1 shows the particle-size distribution envelopes of the two layers.

The area is arid, and the groundwater table fluctuates seasonally. The pore pressure below the groundwater table is hydrostatically distributed. Table 1 shows that the depth to the groundwater table varied between the testing occasions between 6.4 and 5.0 m. The groundwater table depths shown in Table 1 were measured by means of a standpipe piezometer with a filter tip placed at a depth of 11 m. Notice that the groundwater table rose during the time between the compression and tension testing.

Figure 2 illustrates the standard penetration test (SPT) index (N-value) obtained from a borehole located 7 m from the test pile. The N-index in the lower layer varied between 12 and 25 blows/0.3 m, with an average of about 15 blows/0.3 m in the 3–11 m zone, which classifies the compactness of the soil to a compact (medium) condition.

Figure 3 presents the results from two friction-jacket cone penetrometer tests put down at a distance of 2.5 m from the test pile. The cone point stress, q_c, is shown in Fig. 3*a*, the local friction, f_s, in Fig. 3*b*, and the friction ratio, f_s/q_c, in Fig. 3*c*. The data are quite scattered. The boundary between the two soil layers is discernible, however. Further, both the cone point stress diagram and the local friction diagram indicate a looser soil at a depth of about 9 m. The average friction ratio in the sand layer between 10.0 m and 12.0 m depth is 2.4%. This value is larger than the ratio normally found in a sand.

Test pile and instrumentation

The test pile was a square, nominally 285 mm diameter, 12.0 m long, precast concrete pile reinforced with four

Printed in Canada / Imprimé au Canada

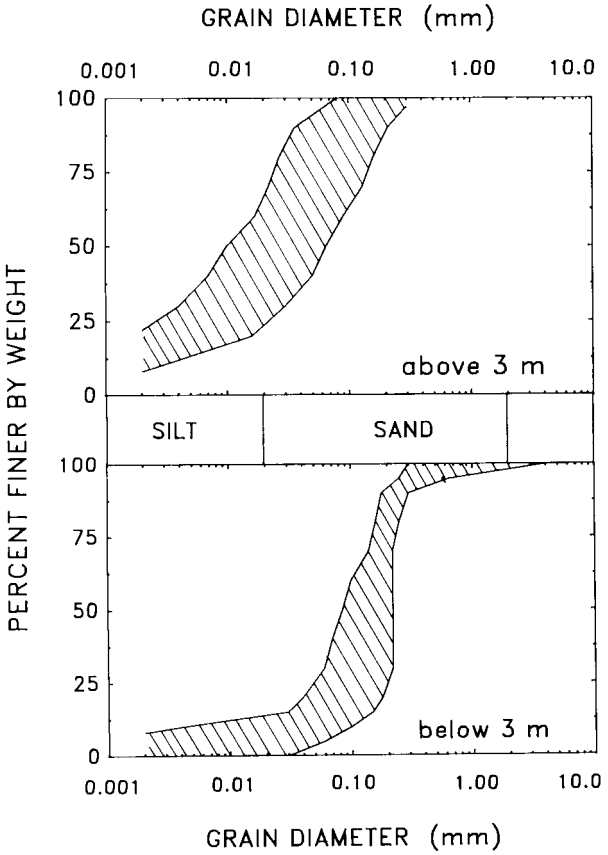

FIG. 1. Particle-size distribution envelopes of the two soil layers.

22 mm bars with a yield strength 420 MPa. The concrete largest aggregate size was 20 mm, and the concrete 28 day cube strength was 45 MPa. The axial tensile strength of a cracked pile section depends only on the strength of the steel reinforcing bars, whose combined strength is about 600 kN. The total weight of the pile is about 20 kN.

The pile was equipped with load cells of a type modified from the original Mustran cell used for instrumentation of cast-in-place piers (Reese *et al.* 1976; Reese 1978). Each cell consisted of a 16 mm diameter, 200 mm long steel bar on which electrical resistance strain gages are affixed. The strain gages were sealed and the bars covered with a watertight rubber hose. The dimensions were designed to give the finished cell an axial stiffness similar to that of concrete.

In the laboratory, the cells work equally well in compression and tension. However, when placed in the pile and subjected to tension they will cease to provide correct load data once the tensile strength of the pile is reached and the concrete starts to crack. Naturally, when a crack occurs near a cell, its calibration is lost and its reading becomes unreliable. For a driven pile, such as the test pile, cracks can also be caused by the driving.

Each cell to be placed in the pile was calibrated in the laboratory under static, repeated, and sustained loading. A straight-line relation was observed between strain and applied load, and no zero-drift was indicated for loads sustained for 48 h.

Before pouring the concrete to make the pile, eight cells were placed inside the reinforcing cage in the centre of the casting form and parallel with the pile longitudinal axis. The cells were placed at a centre-to-centre spacing between cells

TABLE 1. Dates of testing and groundwater observation

Date	Depth to groundwater (m)	Event
June 17, 1984		Driving of the piles
June 20, 1984		Installation of the piezometer
Aug. 22, 1984	6.20	Compression I
Aug. 29, 1984	—	Compression II
Sept. 13, 1984	6.36	Compression III
Oct. 28, 1984	6.70	
Feb. 5, 1985	5.02	Tension

of 1.5 m, with the lowest cell 0.5 m above the pile toe and the uppermost cell 1.0 m below the pile head. Thus, with the pile embedment length of 11.0 m, the uppermost cell, cell 1, was level with the ground surface.

After pouring and curing of the concrete, no more individual load-cell calibration was made. Instead, cell 1 was used as a benchmark for determining the relation between the measured strain and the load in the pile, that is, a benchmark toward the EA-value of the pile, where E is modulus of elasticity and A is pile cross-sectional area (no resistance acted on the pile between the pile head and cell 1).

Driving data and test arrangement

The reaction to the static loading was obtained from four piles driven before the test pile and to 11 m depth in the corners of a rectangle with long and short sides of 5.0 and 2.5 m, respectively. The test pile was driven in the centre of the rectangle.

The piles were driven on June 17, 1984, by a Delmag D12 diesel hammer. All five piles had a gradually increasing penetration resistance with depth. The test pile penetration resistance at the end of driving was 4 blows/25 mm. No restriking was performed.

The tension test reaction was obtained by means of two hydraulic jacks reacting against a girder resting on concrete blocks on the ground.

The compression tests were conducted by means of a hydraulic jack reacting against heavy beams connected to the four anchor piles. Vertical movements were measured with two diametrically opposed dial gages having a 0.01 mm gradation. The applied load was determined by means of a separate load cell.

Test procedure and pile head load–movement data

The first compression loading test consisted of applying load in increments of 100 kN and maintaining each load level for about 1 h up to a total load of 1000 kN and unloading from this level in decrements of 200 kN.

The second compression loading test was undertaken 1 week after the first (see Table 1) and consisted of reloading the pile in increments of 250 kN to the same maximum load, 1000 kN. Unloading was in decrements of 250 kN.

The third compression loading test was undertaken 2 weeks after the second test. The pile was again loaded in increments of 100 kN. At a load level of 900 kN, the movements became

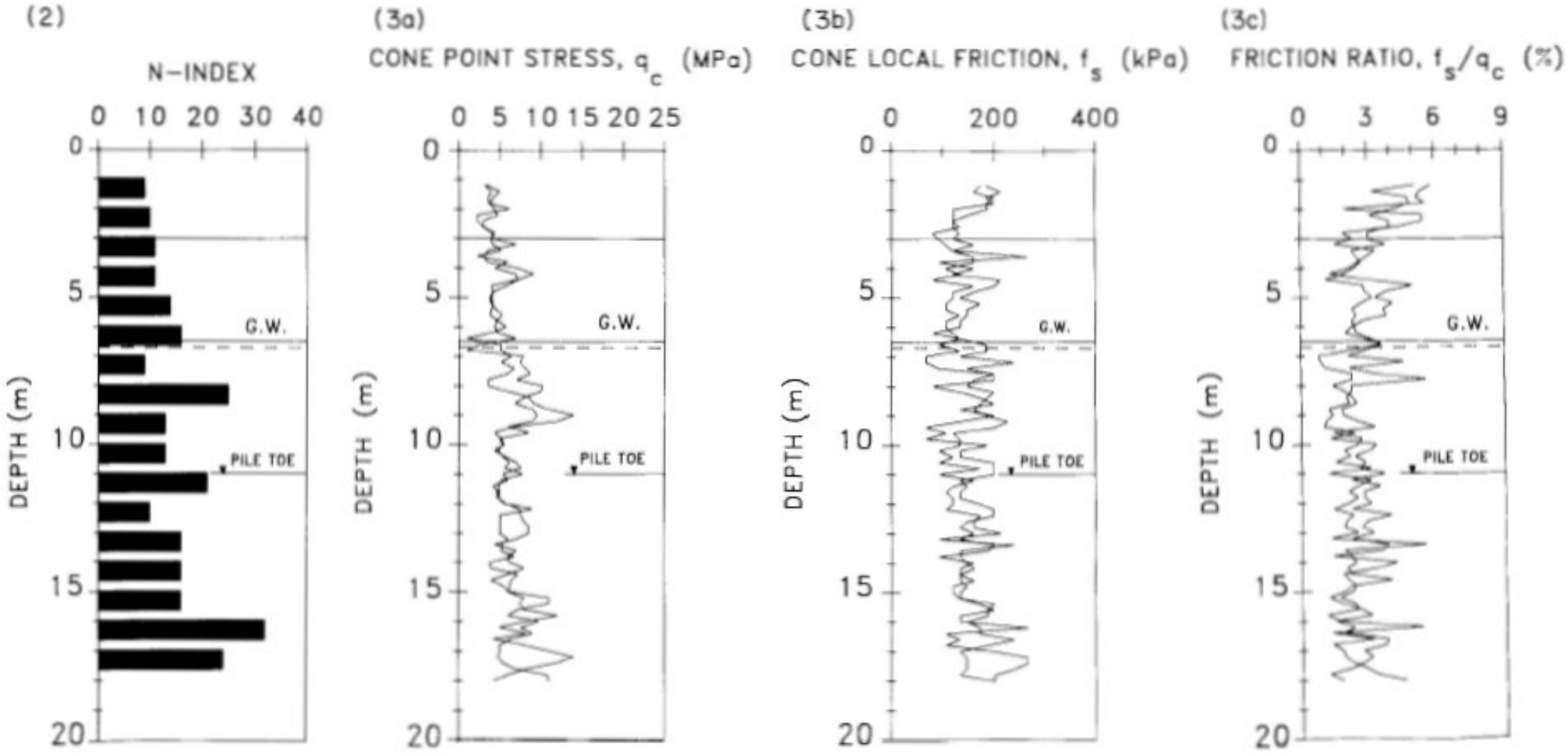

FIG. 2. Standard penetration test profile from a borehole located 7.0 m away from the test pile. FIG. 3. Results from two static cone penetrometer tests 2.5 m away from the test pile: (*a*) cone point stress, q_c; (*b*) cone local friction, f_s; (*c*) cone friction ratio, f_s/q_c.

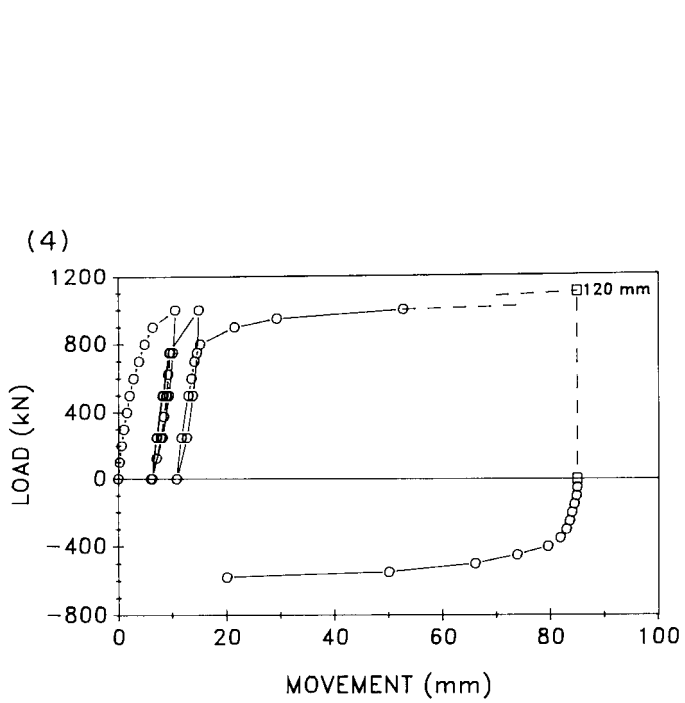

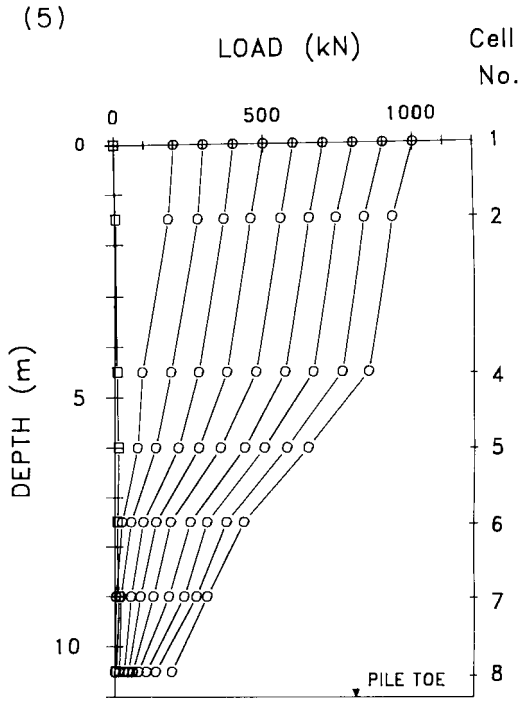

FIG. 4. Pile head load–movement diagram (pile 1). FIG. 5. Load distribution in the pile as measured in test I. □, measured load remaining after full unloading.

progressively larger and the subsequent increments were reduced to 50 kN. The maximum load applied was 1100 kN, which was reached at a pile head movement of 120 mm and could not be maintained.

Five months after the third compression test, a tension test was conducted, with the pile loaded by tension increments of 50 kN. When the applied load had reached 400 kN, movements started to become progressive. The maximum load applied was 580 kN, at which load the upward pile head movement was 65 mm and the load could not be maintained.

Figure 4 presents the load–movement diagram from the four static loading tests. Failure did not occur in the first two loading tests, that is, because full shaft resistance was mobilized, the toe resistance was not fully developed. In the third test, failure occurred between 900 and 1000 kN. In the fourth test, the tension test, failure appears to be starting at about 500 kN and fully developed at 580 kN. It may be noted that the tensile failure load is uncomfortably close to the mentioned tension strength of the reinforcement. However, no cracks were visible in the shaft portion of the pile that was above ground.

Measurement results

The strain recorded by uppermost pile cell, cell 1, was matched to the applied load to calibrate the pile modulus. In the interval between small loads and loads up to 300 kN, the induced strain was a curvilinear function of the load. A strain–load relation was established by curvilinear regression, giving a regression coefficient of 0.999. In the interval between 300 and 1000 kN, the load–strain relation was linear, with a regression coefficient of 0.999.

The pile modulus, E, at the location of cell 1 resulting from the linear relation was 35 GPa. The load in all other pile cells was determined by taking the recorded strain times the EA-value determined from cell 1, where A is the cross-sectional area of the test pile.

The assumption of constant modulus in the pile implants an error, of course, because the pile modulus along the pile must vary. Furthermore, in the saturated zone below the groundwater table, the modulus is expected to have increased beyond the modulus for dry conditions.

In the tension test, the loads rapidly exceeded the tension strength of the concrete. Therefore, the data from the uppermost cell do not correctly represent the conditions for the cells lower down the pile. Although the cells nearest the pile toe received tension loads smaller than the concrete strength, no calibration can be established. Consequently, no reliable calculation of the loads near the pile toe is possible for the tension test.

The strain induced by the loading was determined to one unit of microstrain. One microstrain calibrates to a load of 35 kN. About half of this value is the maximum precision of the data and also the minimum error involved.

One cell, cell 3, did not survive the pile driving, but all other cells worked and provided consistent data. However, the load value obtained from cell 2, located 1.5 m below the ground surface, were consistently smaller than reasonably expected. For example, at the applied load of 1000 kN, cell 2 indicated a load of 937 kN, that is, a shaft resistance of 63 kN, which is an unrealistically high value. (To obtain this amount of shaft resistance in an effective stress analysis (see below), a β-value as high as 3.2 must be assigned to the soil between the ground surface and to a depth of 1.5 m, which is 6–10 times larger than commonly assigned values.) However, in the interest of maintaining a consistent treatment of all measurements, no attempt was made to "correct" the readings taken by cell 2 when plotting the load data.

Figure 5 presents a plot of the loads measured in the test pile during the first compression test. In eyeballing the diagrams, the results appear to suggest that down to a depth of about 7 m, the load in the pile decreases progressively, which means that the unit shaft resistance can be stated to

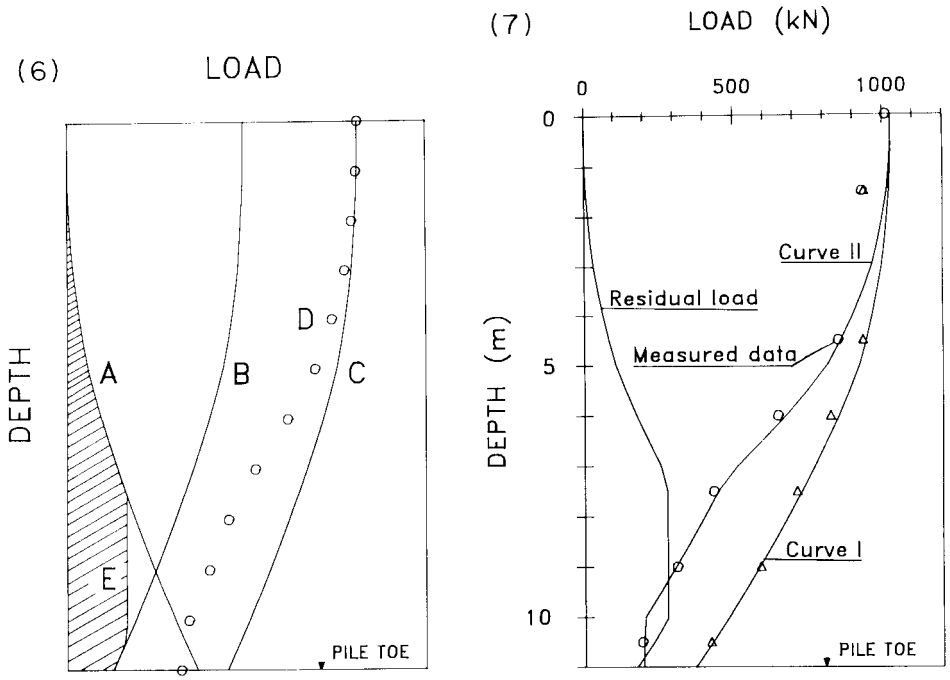

FIG. 6. Principle of determining residual load as to distribution and magnitude in relation to loads induced during the static test.
FIG. 7. Load distributions in the pile during test I, showing the residual load, measured load, calculated true load (curve I), and calculated measured load (curve II).

be approximately proportional to the effective overburden stress. Below about 7 m, the load distribution is linear, which would mean that the unit shaft resistance is constant, that is, the normal stress against the pile is constant and independent of the effective overburden stress. A constant unit shaft resistance is unlikely because it would mean that the basic physical principle of resistance to sliding movement being a function of normal stress is invalid, which would be hard to accept. However, similar results are available in the technical literature, for example, Vesic (1970), Tavenas (1971), and Meyerhof (1976). The *Canadian foundation engineering manual* (Canadian Geotechnical Society 1985) quotes such results and names the depth where the unit shaft resistance becomes constant "the Critical Depth."

Further, the diagram in Fig. 5 implies that the maximum load at the pile toe was about 190 kN. The balance, 810 kN, to the 1000 kN maximum load occurring in the compression test is shaft resistance. The tension resistance is, of course, all shaft resistance. Therefore, the results appear to indicate that the shaft resistance in compression is much larger than the shaft resistance in tension. In contrast with the critical depth "conclusion," this finding does not violate fundamental principles, but is it a correct conclusion?

Theoretical background to the evaluation of the data

In most field testing programmes of instrumented piles in sand reported in the literature (e.g., Vesic 1970; Tavenas 1971), it was assumed that the residual load due to pile installation was negligible. Therefore, when planning the present study, no attempt was made to measure the residual load resulting from the installation of the test pile, and all gages were zeroed before commencing each loading test.

A preliminary analysis of the field test data using a bearing capacity equation gave an apparent toe bearing capacity factor of about 10. The toe bearing capacity factor calculated in this way is much smaller than any value reported in the literature for piles driven in sand. This discrepancy raised questions about the validity of the assumption that the residual load due to pile installation was negligible. Furthermore, the unit shaft resistance obtained from the measured test data was a function of the overburden stress only at shallow depth. Deeper down, it appeared to be about constant, suggesting the presence of a critical depth. However, any conclusions drawn from the load distribution shown in Fig. 5 include the mistaken assumption of no load being present in the pile at the start of the test. In fact, the pile is subjected to a considerable load from the soil before any load is applied to the pile head.

As stated by Fellenius (1984, 1989*a*), because of the stiffness difference between the pile and the soil, there will always be a transfer of load between the pile and the soil whether or not there is a load applied to the pile head. In the upper portion of the pile, load is transferred from the soil to the pile, and in the lower portion the load is transferred from the pile to the soil. At the neutral plane, there is an equilibrium of the load between the two portions. The load transfer is associated with small movements of the soil relative to the pile. As a very small relative movement is sufficient to mobilize the shear strength of the soil, the induced shear forces along the pile can be assumed equal to fully developed shaft resistance. The load induced in the pile is called "residual load."

Fellenius (1989*b*) has presented a method for determining the residual load as to distribution and magnitude from an effective stress calculation of the distribution of ultimate shaft resistance. The method is presented in Fig. 6, showing four load distribution curves in a pile of a certain embedment depth. Curve A, a "resistance curve," is the integration of the shaft resistance along the pile. Because the unit shaft resistance increases *linearly* with depth (it is proportional to the effective overburden stress), the load in the pile

TABLE 2. Values resulting from the calculations

Layer	Depth (m)	Dry density (kg/m^3)	Actual total density (kg/m^3)	β	N_t
Silt–sand	0.0–3.0	1600	1600	0.40	—
Dry sand	3.0–5.0	1800	1800	0.50	—
Moist sand	5.0–6.5	1800	1900	0.65	—
Saturated sand	6.5–11.0	1800	2000	0.65	30

increases *progressively* with depth. Curve B, a "load curve," represents the load distribution in the pile *immediately* after applying a load to the pile head. The load is equal to the total shaft resistance according to curve A plus a small toe resistance. The intersection between curves A and B indicates the neutral plane or point of equilibrium between, on the one hand, the negative shaft resistance above the neutral plane and, on the other hand, the positive shaft resistance below the neutral plane plus the toe resistance. The shaft resistance is fully developed, but, because the movements are very small, the toe resistance is only partially developed.

In reality, nature will not accept sudden changes and, therefore, the sharp change from curve A to curve B occurs over a transition length. Fellenius (1989*b*) constructs this by means of a vertical line marked E in Fig. 6. The residual load in the pile is then the shaded area between curve A, line E, and curve B. That line E is vertical means that no residual shear acts in the transition zone, that is, the residual load does not change along this length of the pile.

In a static loading test to failure, all the shaft resistance acts in the positive direction and the toe resistance is fully developed. The load distribution is then according to curve C, which is parallel to curve B.

If the pile is equipped with gages to measure load and the gages are assumed to read zero before the test, then data points D will be plotted from the measurements. A curve through points D can be obtained from curve C, the true load distribution in the pile, when subtracting the residual load represented by the shaded area.

To analyze test data, one starts with assuming a shear strength distribution along the pile, a residual toe load, and a pile toe resistance. These assumptions govern the residual load in the pile, and when adding the residual load to the measured load values, a load distribution is determined which is then compared to the assumed values. The process is iterative and, through a trial and error approach selecting different soil parameters and residual load values, a final solution is obtained wherein measured and calculated load distributions agree.

Analysis of the test data

Assessment of capacity distribution on shaft and toe resistance by means of wave equation analysis

A wave equation analysis has been performed by means of the GRLWEAP program (Goble, Rausche, and Likins Inc. 1990) with input values of quake, damping, and hammer characteristics as recommended in the GRLWEAP manual for sand soils. The program was run with a linearly increasing unit shaft resistance, with a total shaft resistance of 400 kN chosen low to represent the temporary breakdown of static shaft resistance occurring during initial driving in most soils.

The capacity developed in the test agrees reasonably well with the capacity computed by the wave equation analysis. For the observed penetration resistance of 4 blows/25 mm, the bearing graph obtained by means of the wave equation analysis indicated an ultimate resistance in the range of 700–800 kN, that is, a toe resistance ranging from 300 through 400 kN. When repeating the analysis with the toe quake value increased from the manual recommended value of 2.5–5.0 mm and reducing the value of hammer efficiency from 0.72 to 0.6, the computed capacity boundaries decreased by about 100 kN. As soil setup is common also in sand soils, in restriking the pile, the penetration resistance might well have increased to about 5 or 6 blows/25 mm. *Assuming* that the shaft resistance at restrike has increased to 600 kN, the analysis results indicated a capacity in the range of 1000–1200 kN, suggesting a toe resistance in the range of 400–600 kN at the time of the static loading test. The results of the wave equation analysis of the driving data were used as a guide at the outset of the static analysis described below.

Had a restrike been carried out after the static testing, with careful observation of the penetration for the first couple of blows, the wave equation would have been approximately calibrated to the site conditions. Then, wave equation analysis would have become a useful tool in the inspection and quality control in the driving of the construction piles.

Compression tests

For the analysis, an effective stress method, β-method, was applied with the shaft and toe resistance controlled by only the effective overburden stress (no cohesion intercept). The effective overburden stress is a function of the density of the soil at the site. Density was not determined, however, and has to be assumed. The sand layer was taken to consist of three layers with different density, namely, the upper, the lower, and an intermediate layer. The value assumed in the calculations for the upper layer was 1600 kg/m^3, which is dry density, as applicable well above the groundwater table. The lower layer, the sand layer, has a dry density of 1800 kg/m^3 and a total saturated density (applicable below the groundwater table) of 2000 kg/m^3. A density of 1900 kg/m^3 was assigned to the intermediate layer, a 1.2 m thick zone above the groundwater table, to account for partially saturated soil.

The β-values that resulted from the iterative calculations are compiled in Table 2. The table also includes the toe bearing capacity coefficient, N_t, resulting from the calculations. The calculations were performed by means of the UNIPILE program (Goudreault and Fellenius 1990). No compensation for the buoyant pile weight (13 kN) was included.

Table 2 does not include any change in β-value in the saturated sand above and below the 9 m depth despite a change in strength suggested by the static cone penetrometer data. Attempts were made to fit the theoretical distributions to the measured loads using a higher β-value in the upper 1.5 m and a lower value below 9 m, but no good fit was accomplished. Furthermore, it was not possible to achieve the fit by applying a smaller β-value when calculating negative shaft resistance than when calculating positive shaft resistance.

The values in Table 2 resulted in a calculated total capacity of 1027 kN, made up of 667 kN of shaft resistance and

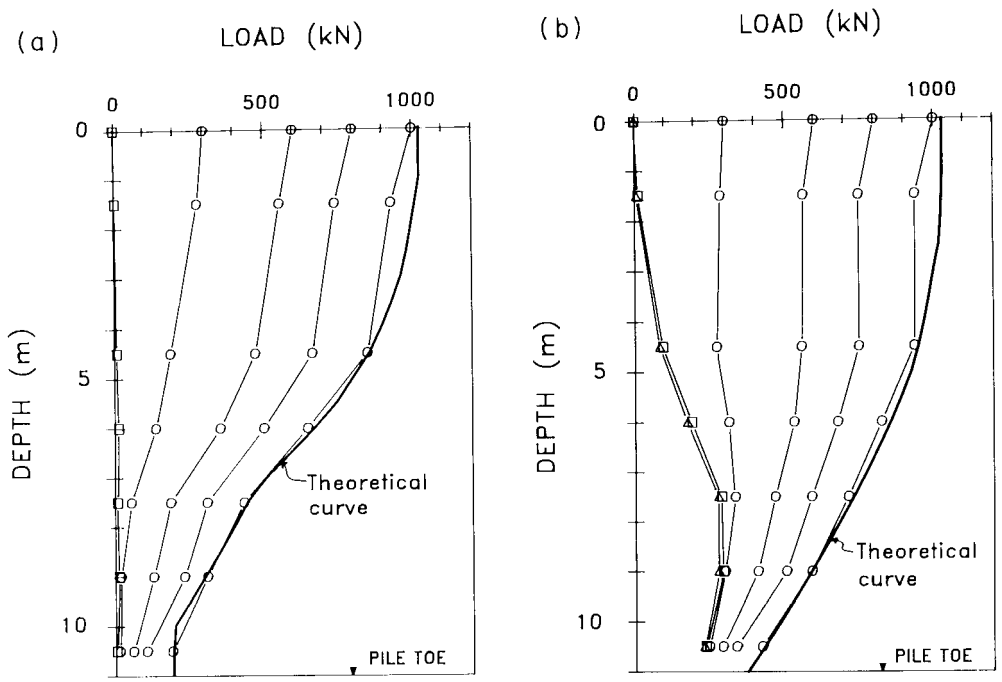

FIG. 8. Test I load distribution (*a*) without the correction for residual load, and (*b*) with the correction for residual load. ○, measured load remaining after full unloading; △, calculated residual load before the start of the test.

360 kN of toe resistance. Figure 7 presents the theoretical "true" load distribution in the pile, curve I. The diagram also shows measured load value (circles), the distribution of residual load determined according to the principle given in Fig. 6 and a residual toe resistance of 170 kN with the residual positive shaft resistance (curve B in Fig. 6) calculated using the same β-values, the vertical portion (line E in Fig. 6) matched to the measured load values, and a curve, curve II, representing the theoretical "measured" load distribution.

The curves shown in Fig. 7 are unique. That is, only the values given in Table 2 will satisfy the conditions that the same unit shaft resistance be used for both the residual load and the load distribution in fitting the calculated "measured" load distribution to the actually measured load values. Changing the β-values in the moist and saturated sands by more than 0.02 up or down and (or) the N_t-value by more than 2 units will destroy the fit.

As mentioned, the measured load values include small errors and are only correct within, perhaps, 20 kN. Furthermore, the density values are only correct within about 100 kg/m^3. Therefore, the β-values given in Table 2 are only reliable within the first decimal and the N_t-value within a few units.

The β-values in Table 2 agree well with recommendations given for design by Fellenius *et al.* (1989*a*). The N_t-value of 30 is smaller than the recommendation, however. It is of interest to note that the ratio between th β-value at the pile toe and the N_t-value is 2.2%, which is very similar to the static cone penetrometer friction ratio of 2.4%.

The primary result of the analysis, however, is not the actual β- and N_t-values but the clear indication that the pile is subjected to residual load and that neglecting this in any evaluation of the test data would result in completely erroneous conclusions from the test results.

Figures 8–10 present the test data for all three tests without and with the correction for residual loads established from the first test. The diagrams have been supplemented with the calculated "measured" load curve (Figs. 8*a*, 9*a*, 10*a*) and with the calculated distributions of "true" load and residual load (Figs. 8*b*, 9*b*, 10*b*). No attempt was made to adjust to the obvious fact that the first test changed the residual load in the pile for the second test, and the second test again changed the residual load in the pile for the third test. The changes consist mainly of increased residual toe resistance and are indicated in the diagrams by the progressive loss of agreement between the data of the second and third tests and the distributions calculated for the first test.

TABLE 3. Gross and net pile head movements

	Per test		Accumulated	
	Gross (mm)	Net (mm)	Gross (mm)	Net (mm)
Test I	10.5	6.0	10.5	6.0
Test II	14.8	10.7	20.8	16.7
Test III	52.7	—	63.4	—

The gross pile head movement at the applied load of 1000 kN and the net after unloading are presented in Table 3.

The compression of the pile is small in relation to the movement of the pile. When combining the load distributions for the applied load of 1000 kN for the three tests with the elastic modulus of 35 GPa, the compression of the pile induced by the test load calculates to about 2 mm. Deducting the pile compression from the pile head movement indicates that the gross and accumulated toe movement at tests I–III for the applied load of 1000 kN was about 8, 19, and 61 mm, respectively, or in relation to the pile diameter: 4, 7, and 18%, respectively. Obviously, the toe movement in the first two tests was not large enough to mobilize fully the toe capacity.

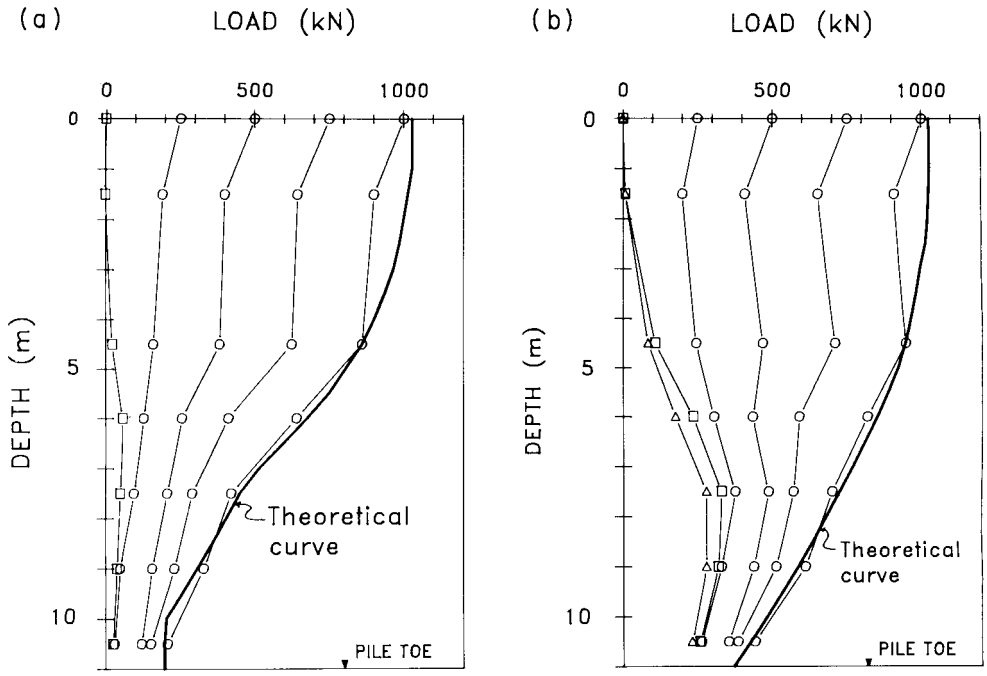

FIG. 9. Test II load distribution (*a*) without the correction for residual load, and (*b*) with the correction for residual load. The residual load is that from before test I. □, measured load remaining after full unloading; △, calculated residual load before the start of test.

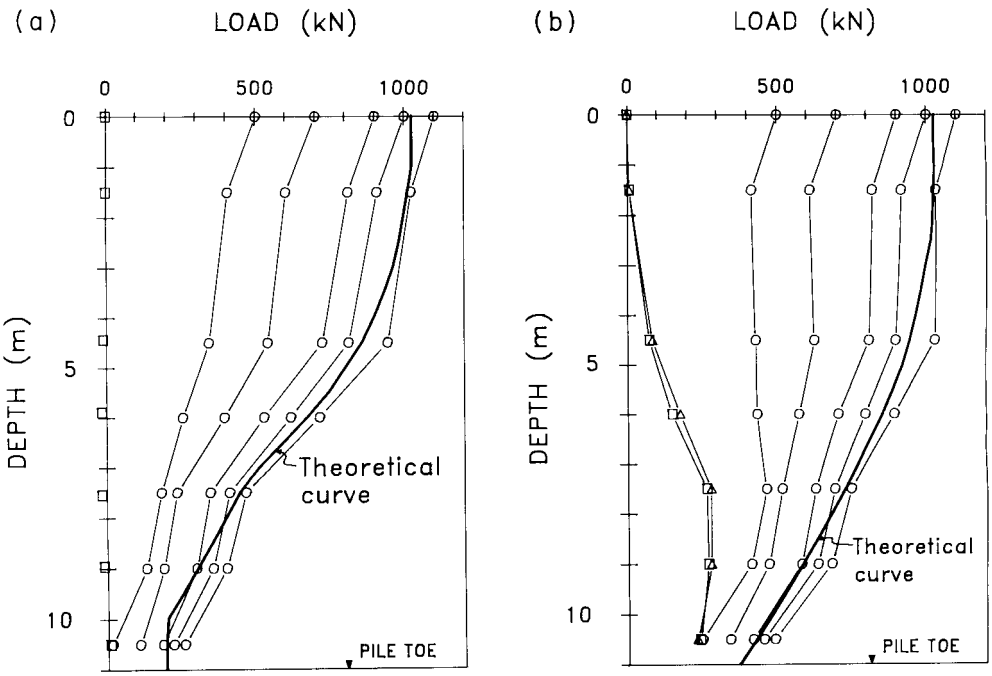

FIG. 10. Test III load distribution (*a*) without the correction for residual load, and (*b*) with the correction for residual load. The residual load is that from before test I, and the theoretical distribution curves relate to the 1000 kN applied load, although the data for 1100 kN applied load are also included in the diagrams. □, measured load remaining after full unloading; △, calculated residual load before the start of test.

As judged from Fig. 4, the load–movement diagram, failure had not occurred in the first test at the applied load of 1000 kN. Yet, in the third test, the pile clearly failed at the 1000 kN load. However, the first test had almost reached failure and a small increase of the load would probably have showed this. In the third test, the shaft resistance had deteriorated somewhat, and the toe resistance was apparently engaged already before the start of the test. Consequently, the pile reached failure at 1000 kN load.

Tension test

At the time of the tension test, the groundwater table had risen to a depth of 5.02 m. The rise resulted in a reduced effective stress. The calculated reduction of shaft resistance due to the subsequent reduction in effective stress is 60 kN, and the new shaft resistance is 607 kN. This value is higher than the tension capacity of 500–580 kN. The difference can be explained by degradation of the shaft resistance induced by the compression tests. However, the tested tension capacity

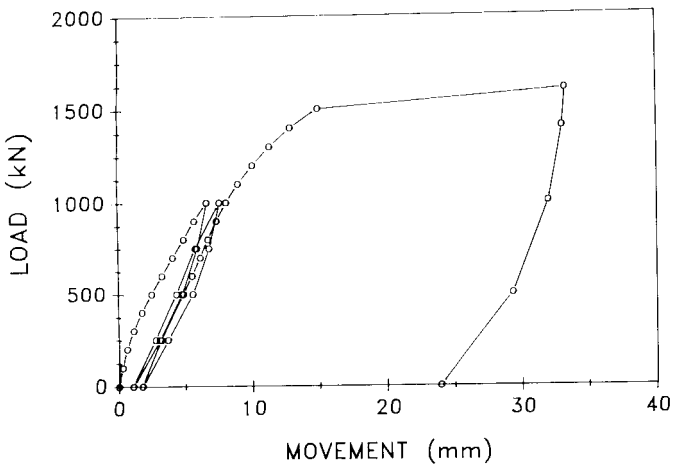

FIG. 11. Pile head load–movement diagram (pile 2).

is very much in doubt, as mentioned above, and the apparent smaller tension resistance cannot be taken as any reliable indication that the negative shaft resistance is smaller than the positive shaft resistance.

The rise of the groundwater table from a low of at least 6.7 m on October 28 to 5.0 m measured at the time of the tension test on February 5 (Table 1) caused a reduction in effective stress of 17 kPa. This unloading of the soil must have resulted in a slight expansion of the sand. Considering a probable elastic modulus of 100 MPa for the sand, the expansion would be a movement of about 0.2 mm/m in the saturated sand, accumulating up and down from the neutral plane. This movement is small, but although it is too small to change the direction of the forces along the pile, it must have had some reducing influence on the residual load in the pile. The actual amount of the reduction, however, is not known.

Confirmation test

To verify the analysis results, a second test pile, pile 2, identical to the first test pile, pile 1, but driven 4 m deeper (embedment 15.0 m), was installed 5.0 m from the first pile and tested in an identical procedure. The first two stages (with 4 weeks interval between the tests) consisted of loading the pile in increments of 100 kN to a maximum load of 1000 kN and unloading. In the third stage, 1 week after the second stage, the pile was loaded to failure. The maximum load was 1600 kN, and failure occurred when increasing the load from 1500 to 1600 kN. Figure 11 presents the load–movement diagram from the tests on pile 2.

The β-values and N_t-coefficient given in Table 2 were applied unchanged to the longer pile and used to calculate (by means of the UNIPILE program) the capacity of the pile. The calculated capacity was 1650 kN, which agrees well with the capacity found in the static loading test.

Conclusions

The procedure recommended by Fellenius (1989*b*) for using an effective stress analysis to determine the distribution of residual load in an 11.0 m long instrumented test pile was successfully applied to the test data, proving that the pile was subjected to residual load.

The data were corrected for residual load, and the β-values and the toe bearing capacity coefficient in the soil at the site were determined.

Without the correction for residual load, considerable errors in the evaluation of the test results with regard to shaft and toe resistances would have resulted. As for toe resistance, the error would have been 50% too low, i.e., 190 kN instead of 360 kN, which is due to the neglect of a residual toe load of 170 kN.

The analysis indicated no difference between shaft resistance in tension and that in compression.

Once the residual load was added to the measured loads, no critical depth was discernible.

The same β-ratios and N_t-factor (Table 2) were applied to the results of compression tests on a second test pile, a 15 m long identical pile, and the calculated capacity agreed with the capacity found in the static loading test, suggesting that the procedure of evaluation applied to the first test has general validity.

Acknowledgements

The experimental part of this research was jointly sponsored by the State Contracting Company for Piling and Foundation (SCCPF) of Iraq and the Building Research Center (BRC) of the Iraqi Scientific Research Council. Mr. Hussain U. Bahia and Mr. Ali H. Khalil of the BRC were members of the research team throughout the experimental part of this work. Mr. Safaa Sahib, site engineer of the SCCPF, and Mr. Adil H. Alsaffar, researcher at the BRC, deserve credit for assisting in the laboratory and field preparations. Dr. Laith I. Namiq, Dean of the Engineering College, University of Baghdad, permitted access to the university laboratories. The numerical part of this work was carried out at the University of Ottawa, Department of Civil Engineering, and was financially supported by the Natural Sciences and Engineering Research Council of Canada. The analyses were carried out using the main computer of the University of Ottawa.

Canadian Geotechnical Society. 1985. Canadian foundation engineering manual. 2nd ed. Canadian Geotechnical Society, Technical Committee on Foundations, BiTech Publishers, Vancouver, B.C.

Fellenius, B.H. 1984. Negative skin friction and settlement of piles. Proceedings, 2nd International Seminar, Pile Foundations, Nanyang Technological Institute, Singapore.

Fellenius, B.H. 1989*a*. Unified design of piles and pile groups. Transportation Research Board, 1169, pp. 75–82.

Fellenius, B.H. 1989*b*. Prediction of pile capacity. *In* Proceedings of the American Society of Civil Engineers, Geotechnical Engineering Division, 1989 Foundation Engineering Congress, Symposium on Predicted and Observed Behavior of Piles. *Edited by* R.J. Finno. ASCE Geotechnical Special Publication 23, pp. 293–302.

Goble, Rausche, and Likins Inc. 1990. GRLWEAP. Wave equation analysis of pile driving. User's manual, vols. I–IV. Goble, Rausche, and Likins Inc., Cleveland.

Goudreault, P.A., and Fellenius, B.H. 1990. Unipile version 1.0 user's manual. Bengt Fellenius Consultants Inc., Ottawa, Ont.

Meyerhof, G.G. 1976. Bearing capacity and settlement of pile foundations. The eleventh Terzaghi lecture. ASCE Journal of the Geotechnical Engineering Division, **102**(GT3): 195–228.

Reese, L.C. 1978. Design and construction of drilled shafts. ASCE Journal of the Geotechnical Engineering Division, **104**(GT1): 95–116.

Reese, L.C., Touma, F.T., and O'Neill, M.W. 1976. Behavior of drilled piers under axial loading. ASCE Journal of the Geotechnical Engineering Division, **102**(GT5): 493–510.

Tavenas, F.A. 1971. Load tests results on friction piles in sand. Canadian Geotechnical Journal, **8**: 7–22.

Vesic, A.S. 1970. Tests on instrumented piles. Ogeechee River site. ASCE Journal of the Soil Mechanics and Foundations Division, **96**(SM2): 561–584.